Electronic supplementary materials *Mendeleev Commun.*, 2025, **35**, 183–186

Photosensitizing effect of benzene oxidation intermediates on the action spectra of Bi_2WO_6/TiO_2-N composites

Maria E. Morozova, Mikhail N. Lyulyukin, Dmitry S. Selishchev and Denis V. Kozlov

S1 Photocatalyst synthesis

The synthesis of samples was performed according to the previously published methods [S1,S2] of titanyl sulfate hydrolysis with ammonia solution and hydrothermal treatment of the as-obtained nitrogen-doped titania for creation of bismuth-containing composites. The bismuth tungstate calculated content was 8, 14, 20, 30 mass% of the composite sample considered.

S2 Catalyst characterization

The samples were characterized by UV-Vis diffuse reflectance spectroscopy. UV-Vis spectra were recorded on a Cary 300 spectrophotometer equipped with a DRA-30I accessory for measuring diffuse reflections at room temperature with a resolution of 1 nm in the range of 250-850 nm.

The amount of total carbon in the selected samples before and after reaction was analyzed using Analytik Jena multi N/C 3100 duo TOC/TNb analyzer with an external HT 1300 module for solid sample analysis. The amounts of detected carbon in the samples before the start of the reaction were practically null.

S3 Photocatalytic experiments

The samples were tested in a continuous-flow reactor for the photocatalytic oxidation of benzene and cyclohexane vapors under the irradiation from a set of single-peak LEDs. The experimental parameters were as follows: the volume flow rate 0.050±0.001 L min^{-1}, reactor temperature and air relative humidity 40±0.2 ℃ and 20±1%. To monitor periodically the changes in the gas phase the experimental set-up was connected to Bruker Vector 22 FTIR spectrometer (USA). The concentrations of benzene and cyclohexane were adjusted to be at a constant level of 2 and 40 μ L^{-1} respectively during the experiment. The concentration points were chosen based on the previous experimental data due to the limitations associated with the adsorption of reagents. CO_2 generation rate was selected for the measure of activity. All LEDs were used as adjusted to the photon flux of 1.5 10^{17}photons s^{-1} (i.e., 0.25 μE $s^{-1,}$ or 15 μE min^{-1}). The photonic efficiency during benzene and cyclohexane photocatalytic oxidation is calculated as the ratio of activity value (CO_2 generation rate, μmol min^{-1}) to the total flux of photons incident onto the surface of catalyst per time interval (μE min^{-1}). Other experimental details are presented elsewhere [S3–S5].

To obtain samples with benzene oxidation intermediates, TiO_2-N and 30% Bi_2WO_6/TiO_2-N samples were exposed to radiation with density 100 mW cm^{-2} at a wavelength of 440 nm from LED and benzene vapors with a concentration 10 μ L^{-1} for 15 hours.

S4 Stability of activity (photostability toward cyclohexane and benzene)

The stability of the catalyst is an important factor in describing its activity. This experimental characteristic of sample describes the behavior of sample under the light irradiation and reaction condition during time. In case of benzene and cyclohexane oxidation, it can be the main illustration of the accumulative nature with the stationary reaching of observed processes features. To confirm the stationarity of processes and the positive influence of composite creation effect, we provide activity versus time for samples of this study in Figure S1.

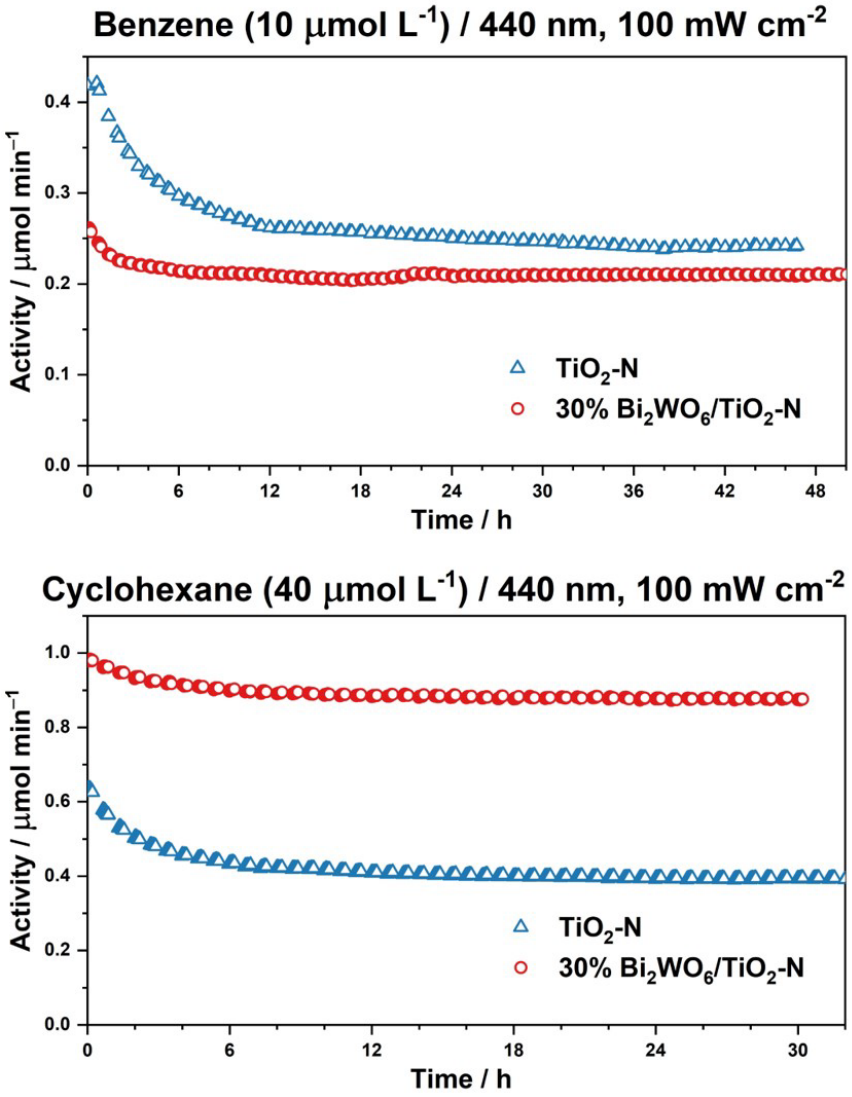

Figure S1. Activity of TiO_2-N and 30% Bi_2WO_6/TiO_2-N samples versus time

TiO_2-N activity decreases during 18 and 6 hours for benzene and cyclohexane oxidation, respectively. There is a combination of factors associated with a degradation of impurity level, which was previously observed during acetone photooxidation.[S1] In the case of benzene, this process is

combined with a formation of aromatic ring containing radicals, as mentioned in the Communication text. These polymer-like intermediates can absorb the incident light, but also they block active sites that lead to a decrease of the conversion rate. When the Bi_2WO_6 is added, the heterojunction between semiconductors is formed and a transfer of photogenerated charge carriers is observed. Consequently, this leads to a faster stationarity reaching and, in the case of cyclohexane oxidation, to an increase in activity. But it is necessary to note that over time a steady-state flow of all processes on photocatalyst surface is achieved and the stable amount of carbon deposits is reached for each case. For example, accumulation of carbon-containing deposits for TiO_2-N is presented on Figure S2.

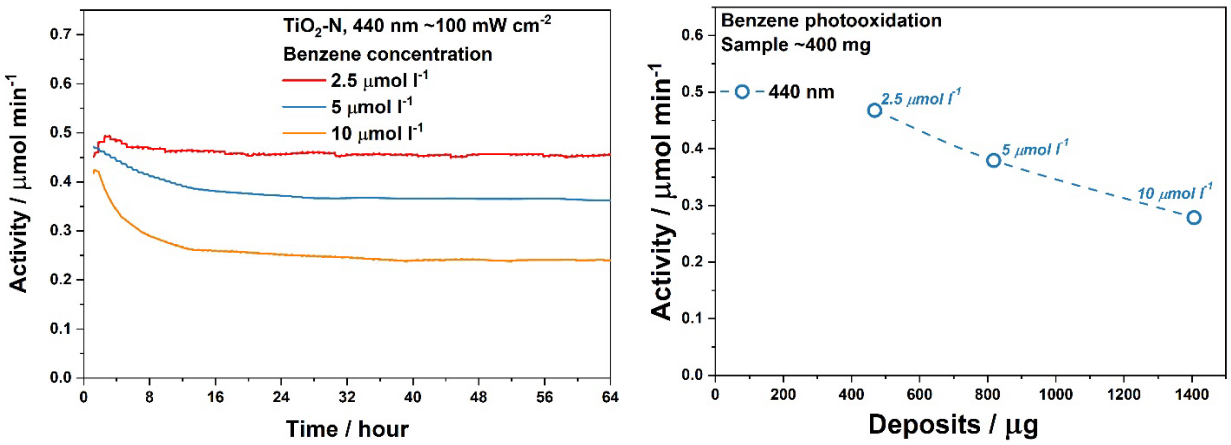

Figure S2. Activity of TiO_2-N and 30% Bi_2WO_6/TiO_2-N samples versus time

After the benzene supply is turned off, carbon deposits will be oxidized under the incident photon flux until the surface is cleaned.

S5 IR spectra

Some characteristical lines may be shown for TiO_2 in accordance with the literature data:

- 1256 – adsorbed benzene ring[S6]
- 1335 – adsorbed benzene ring[S7]
- 1427 – stretching of C-O[S8]
- 1480 – adsorbed benzene ring[S6, S9]
- 1659 – adsorbed benzene ring[S6, S10]
- 1717 – stretching of C=O[S8]

The surface of the photocatalysts was studied by IR spectroscopy (Figure S3) in an open cell before and after the main experiments due to experimental limitations. This is partly why the severity of the characteristic lines and the observed noises may differ from the ideal ones. However, even from such spectra, after the oxidation of benzene on TiO_2-N, there is an increase in absorption in some positions when compared with the TiO_2-N sample after the oxidation of cyclohexane. The spectra were taken relative to the sample before the oxidation reaction. A difference in spectra is also observed for

the Bi_2WO_6/TiO_2-N sample. More precisely, there is an additional absorption at position 1691 (which is not present for benzene), and an absorption band of 1360-1410, which is not present in the sample after cyclohexane (but it is present in the sample after benzene oxidation). It is worth noting that the positions of the absorption bands for the compared groups may differ markedly for the Bi_2WO_6/TiO_2-N sample from the TiO_2-N sample due to the significantly different structure of these semiconductors and the morphology of their surfaces.

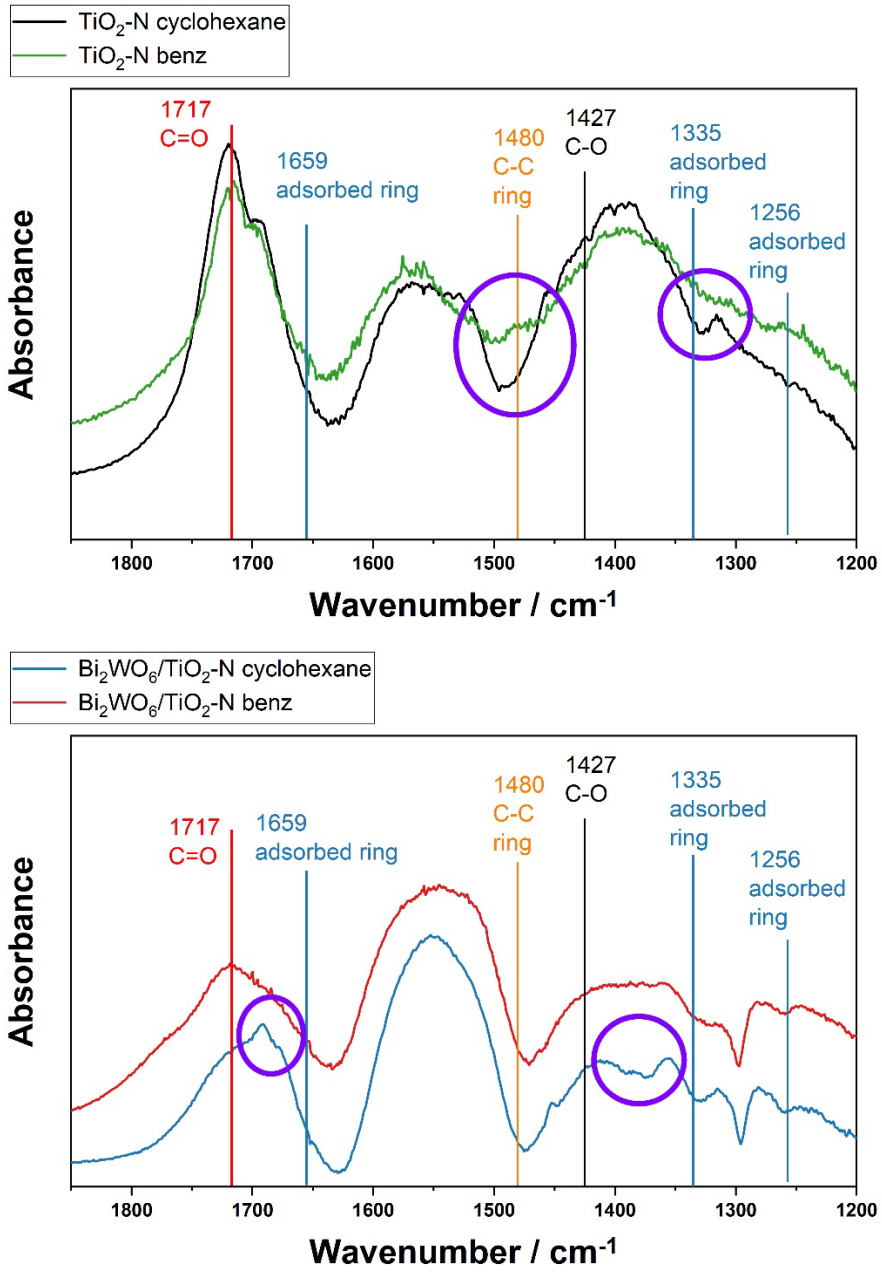

Figure S3. IR spectra for TiO_2-N and 30% Bi_2WO_6/TiO_2-N samples cyclohexane and benzene oxidation. Normalized to samples before reaction

S6 UV-Vis DRS after benzene and cyclohexane photooxidation

To confirm the significant photosensitizing effect of carbon deposits only during the process of benzene oxidation, we present the light absorbance spectra for samples as a Kubelka-Munk function

after both reactions in Figure S4. Changes in the spectra of samples after the reaction of cyclohexane oxidation are also observed. Nevertheless, this effect is insignificant to claim the photosensitization of catalyst surface in the case of cyclohexane oxidation.

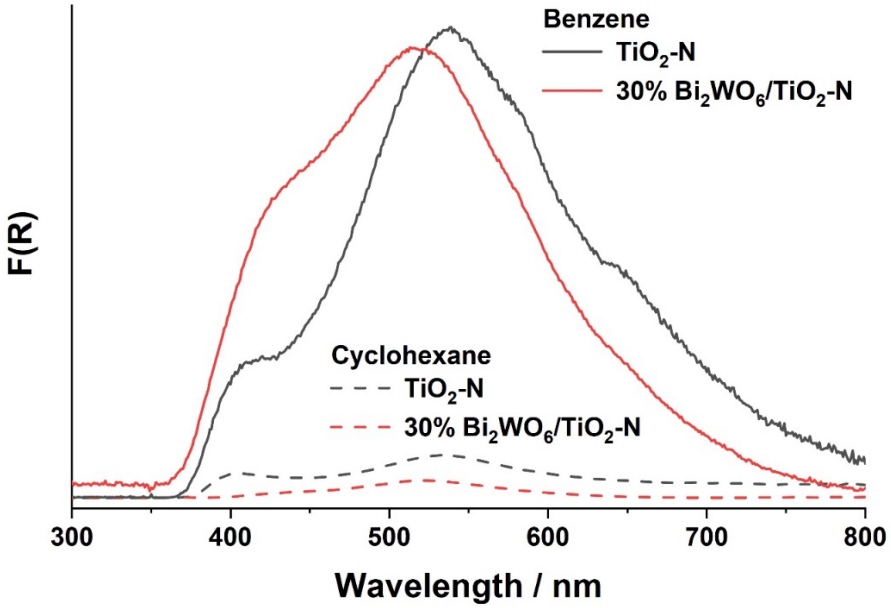

Figure S4. Absorbance for TiO_2-N and 30% Bi_2WO_6/TiO_2-N samples after benzene and cyclohexane oxidation reaction (baseline – the sample before reaction)

References

S1 N. Kovalevskiy, D. Svintsitskiy, S. Cherepanova, S. Yakushkin, O. Martyanov, S. Selishcheva, E. Gribov, D. Kozlov, D. Selishchev, *Nanomater.*, 2022, **12 (23)**, 4146; https://doi.org/10.3390/nano12234146.

S2 M. N. Lyulyukin, M. E. Morozova, D. A. Polskikh, I. P. Prosvirin, S. V. Cherepanova, D. S. Selishchev, D. V. Kozlov, *J. Struct. Chem.*, 2024, **65 (2)**, 341–354; https://doi.org/10.1134/S0022476624020124.

S3 M. Lyulyukin, N. Kovalevskiy, D. Selishchev, D. Kozlov, *J. Photochem. Photobiol., A*, 2021, **405**, 112981; https://doi.org/10.1016/j.jphotochem.2020.112981.

S4 M. N. Lyulyukin, N. S. Kovalevskiy, E. A. Fedorova, D. S. Selishchev, D. V. Kozlov, *Mendeleev Commun.*, 2022, **32 (2)**, 278–280; https://doi.org/10.1016/j.mencom.2022.03.042.

S5 N. S. Kovalevskiy, M. N. Lyulyukin, D. V. Kozlov, D. S. Selishchev, *Mendeleev Commun.*, 2021, **31 (5)**, 644–646; https://doi.org/10.1016/j.mencom.2021.09.017.

S6 K. Hadjiivanov, D. Klissurski, G. Busca, V. Lorenzelli, *J. Chem. Soc., Faraday Trans.*, 1991, **87 (1)**, 175–178; https://doi.org/10.1039/FT9918700175.

S7 M. Nagao, Y. Suda, *Langmuir*, 1989, **5 (1)**, 42–47; https://doi.org/10.1021/la00085a009.

S8 X. Liu, Y. Zhang, S. Matsushima, H. Hojo, H. Einaga, *Chemical Engineering Journal*, 2020, **402**, 126220; https://doi.org/10.1016/j.cej.2020.126220.

S9 W.-C. Wu, L.-F. Liao, C.-F. Lien, J.-L. Lin, *Phys. Chem. Chem. Phys.*, 2001, **3 (19)**, 4456–4461; https://doi.org/10.1039/b104926g.

S10 J.-M. Kim, K. Vikrant, T. Kim, K.-H. Kim, F. Dong, *Chemical Engineering Journal*, 2022, **428**, 131090; https://doi.org/10.1016/j.cej.2021.131090.